Correlation Plenoptic Imaging

Milena D'Angelo,[1,2,*] Francesco V. Pepe,[3,2,†] Augusto Garuccio,[1,2] and Giuliano Scarcelli[4]

[1]*Dipartimento Interateneo di Fisica, Università degli studi di Bari, I-70126 Bari, Italy*
[2]*INFN, Sezione di Bari, I-70126 Bari, Italy*
[3]*Museo Storico della Fisica e Centro Studi e Ricerche "Enrico Fermi," I-00184 Roma, Italy*
[4]*Fischell Department of Bioengineering, University of Maryland, College Park, Maryland 20742, USA*

Plenoptic imaging is a promising optical modality that simultaneously captures the location and the propagation direction of light in order to enable three-dimensional imaging in a single shot. However, in standard plenoptic imaging systems, the maximum spatial and angular resolutions are fundamentally linked; thereby, the maximum achievable depth of field is inversely proportional to the spatial resolution. We propose to take advantage of the second-order correlation properties of light to overcome this fundamental limitation. In this Letter, we demonstrate that the correlation in both momentum and position of chaotic light leads to the enhanced refocusing power of correlation plenoptic imaging with respect to standard plenoptic imaging.

Plenoptic imaging (PI) is a technique aimed at capturing information on the three-dimensional light field of a given scene in a single shot [1]. Its key principle is to record, in the image plane, both the location and the propagation direction of the incoming light. The recorded propagation direction is exploited, in postprocessing, to computationally retrace the geometrical light path, thus enabling the refocusing of different planes within the scene and the extension of the depth of field of the acquired image. As shown in Fig. 1(b), PI resembles standard imaging [Fig. 1(a)]; however, a microlens array is inserted in the native image plane and the sensor array is moved behind the microlenses. On the one hand, the microlenses act as imaging pixels to gain the spatial information of the scene; on the other hand, each microlens reproduces on the sensor array an image of the camera lens, thus providing the angular information associated with each imaging pixel [2]. As a result, a trade-off between spatial and angular resolution is built in the plenoptic imaging process.

Plenoptic imaging is currently used in digital cameras enhanced by refocusing capabilities [3]; in fact, in photography, PI highly simplifies both autofocus and low-light shooting [2]. A plethora of innovative applications in 3D imaging and sensing [4,5], stereoscopy [1,6,7], and microscopy [8–10] are also being developed. In particular, high-speed large-scale 3D functional imaging of neuronal activity has been demonstrated [11]. However, the potentials of PI are strongly limited by the inherent inverse proportionality between image resolution and maximum achievable depth of field. Attempts to decouple resolution and depth of field based on signal processing and deconvolution have been proposed in the literature [10–15].

Our idea is to exploit the second-order spatiotemporal correlation properties of light to overcome this fundamental limitation. Using two correlated beams, from either a chaotic or an entangled photon source, we can perform imaging in one arm [16–21], and simultaneously obtain the angular information in the other arm. In fact, the position and momentum correlations at the core of our proposal were demonstrated more than ten years ago by performing separate imaging and diffraction experiments, respectively [18,21]. Here, we devise a physical context where such correlations can be measured and exploited simultaneously to enhance the performances of a practically useful imaging technique, namely, to improve the depth of field of plenoptic imaging. In this Letter, we develop a comprehensive theory of the proposed technique, named correlation plenoptic imaging (CPI), in the case of chaotic light. In particular, we show that the second-order correlation function possesses plenoptic imaging properties (i.e., it encodes both spatial and angular information), and is thus characterized by a key refocusing capability. From a practical standpoint, our protocol can dramatically enhance the potentials of PI, the simplest method of 3D imaging with the present technological means [10,11]. From a fundamental standpoint, the plenoptic application is the first situation where the counterintuitive properties of correlated systems are effectively used to beat intrinsic limits of standard imaging systems. Moreover, the interest in position-momentum correlations goes well beyond imaging and optics, due to their relation with quantum tomography [22,23].

The working principle of CPI is introduced in Fig. 1(c). In PI [Fig. 1(b)] the sensor is divided into *macropixels* of width δ_x, defining the image resolution; a macropixel is made of $N_u^{(p)}$ micropixels per side, of width $\delta < \delta_x$, fixing the directional resolution [1,2]. An array of microlenses of diameter δ_x and focal length F is inserted in front of the sensor for reproducing, within each macropixel, the image of the main camera lens. Hence, each micropixel collects light from a sector of the main lens and encodes
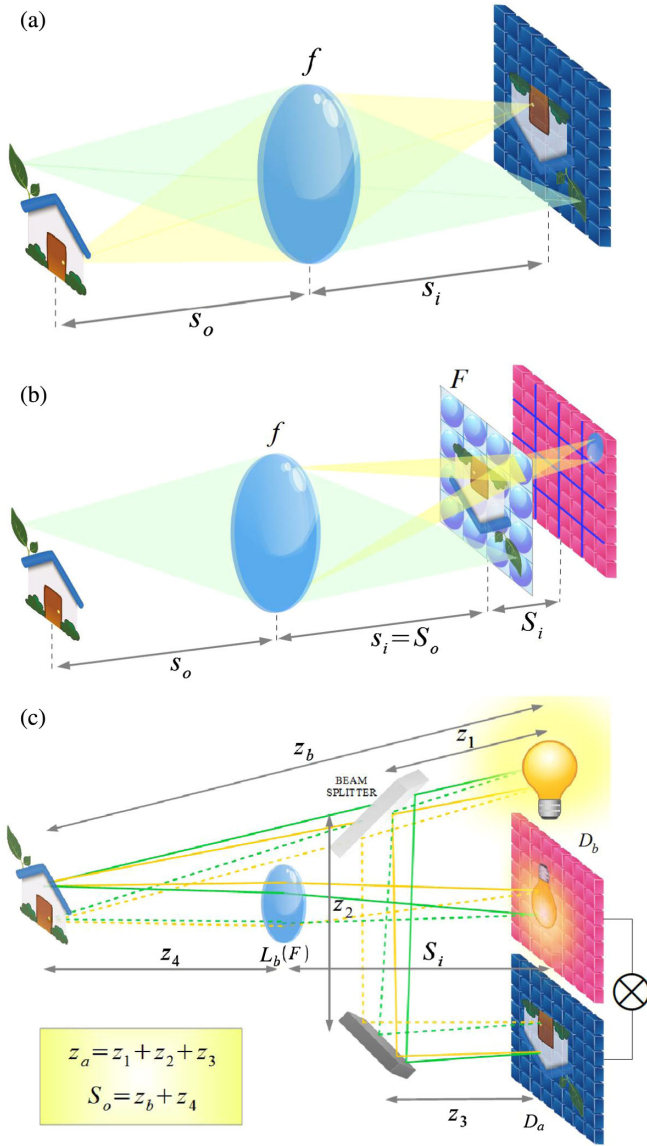
FIG. 1. (a) Standard imaging: The lens focuses the object on the sensor. (b) Plenoptic imaging: The lens focuses the object on a lenslet array; each microlens focuses the main lens on a *macropixel* (blue lines) of the sensor to provide directional information. (c) Correlation plenoptic imaging: By means of correlation measurement, the chaotic light source acts as a focusing element (i.e., as an imaging lens) and enables imaging the object on the (blue) sensor D_a. The light source is imaged by the lens L_b on the (red) sensor D_b to provide directional information. Note: Distances are related by the thin-lens equations: $1/s_0 + 1/s_i = 1/f$, $1/S_0 + 1/S_i = 1/F$.

information on the direction of light that impinges on the specific macropixel, corresponding to a specific point of the acquired image. For a sensor of width W, this configuration yields the following relationship between the number of pixels per side devoted to the spatial ($N_x^{(p)} = W/\delta_x$) and to the directional ($N_u^{(p)} = \delta_x/\delta$) detection of the light field:

$$N_x^{(p)} N_u^{(p)} = \frac{W}{\delta} \equiv N_{\text{tot}}, \qquad (1)$$

where N_{tot} is the total number of pixels per side on the sensor. Simple geometrical considerations indicate that the maximum achievable depth of field is determined by the directional resolution $N_u^{(p)}$; hence, based on Eq. (1), the depth of field can be increased only at the expense of the image resolution $N_x^{(p)}$. In addition, for the direction measurement to be physically meaningful, the image resolution must be well above the diffraction limit, namely, the image pixel size δ_x must be bigger than the minimum image resolution allowed by diffraction.

Now, in CPI [Fig. 1(c)] light is split in two arms, and two sensors are employed: D_a to image the desired scene, and D_b to perform the direction measurement. In fact, when using the correlation properties of chaotic light, the light source plays the role of the focusing element, and can replace the main lens of Figs. 1(a)–1(b) [19,20]. Direction measurement is thus performed by imaging the light source on D_b through the lens L_b, which collects light reflected off the object. Notice that lens L_b replaces the whole lenslet array of Fig. 1(b). As we shall prove, when measuring correlation between D_a and D_b, the image of the desired scene is reproduced on D_a. The image is focused provided the distance z_a between the source and the sensor D_a is equal to the distance z_b between the source and the object [20,24]. Since the two sensors can have the same pixel size δ, and their widths $W_i^{(\text{cp})}$ (with $i = x, u$) are such that $W_x^{(\text{cp})} + W_u^{(\text{cp})} = W$, the number of pixels per side dedicated to the spatial and the directional measurement ($N_i^{(\text{cp})} = W_i^{(\text{cp})}/\delta$, with $i = x, u$) is constrained by the relation

$$N_x^{(\text{cp})} + N_u^{(\text{cp})} = N_{\text{tot}}. \qquad (2)$$

The striking improvement of CPI with respect to PI increases with increasing N_{tot}. Realistic chaotic sources for the realization of the proposed scheme include the pseudothermal sources typically employed in ghost imaging [17,19–21,25], as well as LEDs [26].

Correlation imaging and refocusing.—The core of CPI is the second-order spatiotemporal correlation measurement, as described by the Glauber correlation function [27]

$$G^{(2)}(\boldsymbol{\rho}_a, \boldsymbol{\rho}_b; t_a, t_b) = \langle E_a^{(-)}(\boldsymbol{\rho}_a, t_a) E_b^{(-)}(\boldsymbol{\rho}_b, t_b)$$
$$\times E_b^{(+)}(\boldsymbol{\rho}_b, t_b) E_a^{(+)}(\boldsymbol{\rho}_a, t_a)\rangle, \qquad (3)$$

where $\boldsymbol{\rho}_i$ indicates the planar position on the sensor D_i (with $i = a, b$), t_i is the corresponding detection time, and $E_i^{(\pm)}$ are the positive- and negative-frequency components of the electric field operators at each detector, for which a scalar approximation is assumed. The expectation value in Eq. (3) is evaluated by considering the source statistics. Let us consider a quasimonochromatic chaotic light source characterized by a coherence time larger than $\tau = t_a - t_b$, in such a way that the temporal part of the correlation function can be neglected, and the spatial part reduces to [18]:

$$G^{(2)}(\boldsymbol{\rho}_a, \boldsymbol{\rho}_b) = I_a(\boldsymbol{\rho}_a) I_b(\boldsymbol{\rho}_b) + \Gamma(\boldsymbol{\rho}_a, \boldsymbol{\rho}_b), \qquad (4)$$

where the first term is the mere product of the intensities $I_i = G_{ii}^{(1)}$ at the two detectors ($i = a, b$), and the second term is the nontrivial part of the correlation $\Gamma = |G_{ab}^{(1)}|^2$. Here, $G_{jk}^{(1)}(\boldsymbol{\rho}_j, \boldsymbol{\rho}_k) = C \int d^2q \, g_j^*(\boldsymbol{\rho}_j, \boldsymbol{q}) g_k(\boldsymbol{\rho}_k, \boldsymbol{q})$, with C a constant and $g_i(\boldsymbol{\rho}_i, \boldsymbol{q})$ the Green's function propagating the electric field mode with transverse momentum $\boldsymbol{q}$ from the source to the detector D_i [28]. By propagating the field in the setup of Fig. 1, while assuming for simplicity that lens L_b is diffraction limited, the second term of Eq. (4) yields the desired correlation plenoptic image of the object:

$$\Gamma_{z_a, z_b}(\boldsymbol{\rho}_a, \boldsymbol{\rho}_b) = C' \left| \int d^2\boldsymbol{\rho}_o A(\boldsymbol{\rho}_0) e^{-(i\omega/cz_b)\boldsymbol{\rho}_o \cdot (\boldsymbol{\rho}_b/M)} \right.$$
$$\times \int d^2\boldsymbol{\rho}_s F(\boldsymbol{\rho}_s) G(|\boldsymbol{\rho}_s|)_{\{(\omega/c)[(1/z_b)-(1/z_a)]\}}$$
$$\left. \times e^{-(i\omega/cz_a)[(z_a/z_b)\boldsymbol{\rho}_o - \boldsymbol{\rho}_a] \cdot \boldsymbol{\rho}_s} \right|^2, \quad (5)$$

parametrized by the distances of the sensor D_a (z_a) and the object (z_b). In Eq. (5), C' is a constant, $\boldsymbol{\rho}_o$ and $\boldsymbol{\rho}_s$ are, respectively, the transverse coordinates on the object and the source plane, $A(\boldsymbol{\rho}_o)$ is the aperture function describing the object, $F(\boldsymbol{\rho}_s)$ is the intensity profile of the source, $G(x)_{[y]} = e^{iyx^2/2}$, and $M = S_i/S_o$ is the magnification of the image of the source on D_b. Based on the result of Eq. (5), when the sensor D_a is placed at $z_a = z_b$, for any pixel of the sensor D_b, we obtain

$$\Gamma_{z_b, z_b}(\boldsymbol{\rho}_a, \boldsymbol{\rho}_b)$$
$$\propto \left| \int d^2\boldsymbol{\rho}_o A(\boldsymbol{\rho}_0) e^{-(i\omega/cz_b)\boldsymbol{\rho}_o \cdot (\boldsymbol{\rho}_b/M)} \tilde{F}\left(\frac{\omega(\boldsymbol{\rho}_o - \boldsymbol{\rho}_a)}{cz_b} \right) \right|^2. \quad (6)$$

This result indicates that a *coherent* image of the object $A(\boldsymbol{\rho}_0)$ is retrieved on D_a when measuring correlation with any pixel of D_b; its point-spread function is given by the Fourier transform of the source intensity profile $\tilde{F}(\boldsymbol{\kappa}) = \int d^2\boldsymbol{\rho}_s F(\boldsymbol{\rho}_s) e^{-i\boldsymbol{\kappa} \cdot \boldsymbol{\rho}_s}$. By keeping $z_a = z_b$ and integrating the result of Eq. (6) over the whole detector array D_b, one gets the *incoherent* image of the object, namely

$$\Sigma_{z_b}(\boldsymbol{\rho}_a) := \int d^2\boldsymbol{\rho}_b \Gamma_{z_b, z_b}(\boldsymbol{\rho}_a, \boldsymbol{\rho}_b)$$
$$\propto \int d^2\boldsymbol{\rho}_o |A(\boldsymbol{\rho}_o)|^2 \left| \tilde{F}\left(\frac{\omega}{cz_b}(\boldsymbol{\rho}_o - \boldsymbol{\rho}_a) \right) \right|^2. \quad (7)$$

This is the well-known ghost image produced by chaotic light sources [19,20]. In addition, based on Eq. (5), the correlation measurement between D_b and any pixel of D_a reproduces the image of the source; its point-spread function is given by the Fourier transform of the object aperture function $\tilde{A}(\boldsymbol{q}) = \int d^2\boldsymbol{\rho}_o A(\boldsymbol{\rho}_o) e^{-i\boldsymbol{q} \cdot \boldsymbol{\rho}_0}$, which is

$$\Gamma_{z_b, z_b}(\boldsymbol{\rho}_a, \boldsymbol{\rho}_b)|_{\text{point source}} \propto \left| \tilde{A}\left(\frac{\omega}{cz_b}\left(\bar{\boldsymbol{\rho}}_s + \frac{\boldsymbol{\rho}_b}{M} \right) \right) \right|^2, \quad (8)$$

for a point source placed in $\bar{\boldsymbol{\rho}}_s$. Hence, the one-to-one correspondence between points of the source ($\boldsymbol{\rho}_s$) and points of the sensor D_b ($\boldsymbol{\rho}_b = -M\boldsymbol{\rho}_s$) can only be hindered by diffraction at the object.

In summary, due to the peculiar position and momentum correlation of chaotic sources, the second-order correlation function of Eq. (5) possesses plenoptic properties, namely, it enables the simultaneous measurement of both spatial and angular information. This intriguing result indicates that plenoptic imaging may represent a natural playground for the position and momentum correlations of chaotic sources to find a realistic practical application. In this perspective, it is worth emphasizing that, based on the result of Eq. (8), our scheme may perform plenoptic imaging only when working in the geometrical optics limit. This limit is recovered in both arms of the CPI system when $\lambda z_a/(dD_s) \ll 1$ with d the smallest detail of the object and D_s the width of the source. It is also worth noticing that the diffraction limits on the image and the angular resolution

$$\Delta\rho_a^{\lim} \sim \frac{\lambda z_a}{D_s}, \qquad \frac{\Delta\rho_b^{\lim}}{M} \sim \frac{\lambda z_b}{d}, \quad (9)$$

are defined, respectively, by the characteristic size of the source and the object. Hence, as far as the effects of diffraction are negligible, the spatial and angular resolutions are completely decoupled. The required number of correlation events is the same as in chaotic ghost imaging [29]. We finally remark that the limitations to CPI are ultimately related with fundamental physical constraints (namely, the uncertainty principle) rather than with the geometrical structure of the system.

In view of exploiting the plenoptic properties of the second-order correlation function, let us now consider the more interesting case in which the retrieved image of the scene is out of focus ($z_a \neq z_b$). Inspection of Eq. (5) indicates that the correlation function $\Gamma_{z_a, z_b}(\boldsymbol{\rho}_a, \boldsymbol{\rho}_b)$ incorporates plenoptic information on the light field propagating from the source to the object and the sensors, thus enabling the reconstruction of misfocused images. In fact, as schematically shown in Fig. 2, the propagation direction of the light detected at the point $\boldsymbol{\rho}_a'$ of the sensor D_a can be reconstructed by knowing the source point $\boldsymbol{\rho}_s$ from which it is coming. This reconstruction enables retracing the light path from the source to the correct image plane, which is at a distance $z_b = \alpha z_a$ from the source. Imaging the chaotic source on detector D_b is thus the key feature which enables refocusing in CPI. In fact, from Fig. 2, one can infer the following scaling property:

$$\Gamma_{z_a, z_b}\left(\frac{z_a}{z_b}\boldsymbol{\rho}_a - \frac{\boldsymbol{\rho}_b}{M}\left(1 - \frac{z_a}{z_b} \right), \boldsymbol{\rho}_b \right) \simeq \Gamma_{z_b, z_b}(\boldsymbol{\rho}_a, \boldsymbol{\rho}_b), \quad (10)$$

which is exact in the geometrical optics limit [31]. Similar to PI [2], such a scaling property guarantees the refocusing capability of CPI. Its integral yields the refocused incoherent image
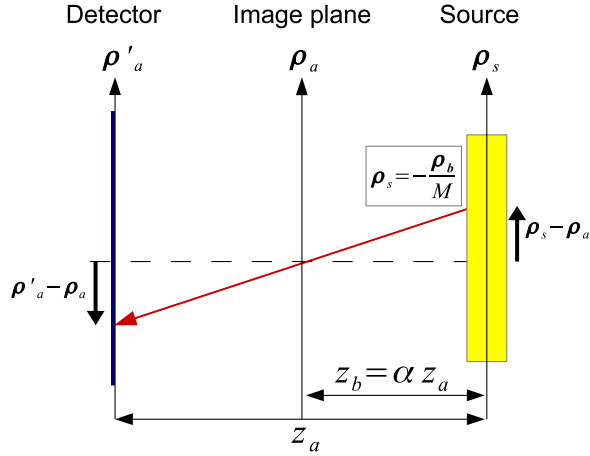
Detector   Image plane   Source

FIG. 2.   Geometrical representation of the scaling property given in Eq. (10), in the case $z_a > z_b$.

$$\Sigma^{\text{ref}}_{z_a, z_b}(\boldsymbol{\rho}_a) := \int d^2 \boldsymbol{\rho}_b \Gamma_{z_a, z_b}\left(\frac{z_a}{z_b}\boldsymbol{\rho}_a - \frac{\boldsymbol{\rho}_b}{M}\left(1 - \frac{z_a}{z_b}\right), \boldsymbol{\rho}_b\right). \quad (11)$$

Figure 3 reports the simulation of CPI for (a) a focused image, (b) an out of focus image taken at $z_b = 5z_a$, and (c) the refocused image obtained by applying the scaling rule of Eq. (11) to the out-of-focus image. We conclude that the correlation properties of chaotic light [18,21] enable achieving a much higher refocusing capability with respect to plenoptic imaging.

The computational steps required for rescaling [Eq. (10)] and integration [Eq. (11)] grow linearly in the total number N_u^2 of angular pixels. Since the operation must be repeated N_x^2 times, the computational steps required for refocusing scale like $(N_u N_x)^2$, as in standard plenoptic imaging. The overall computational time has an additional scaling factor, given by the number of frames which must be averaged to obtain the correlation image.

Depth of focus.—It is worth comparing the performance of PI and CPI in terms of the maximum achievable depth of focus (DOF), namely, the maximum distance from the actual detection plane at which perfect refocusing is allowed. For any plenoptic device, we can define $\alpha = S_i / S_i'$ as the ratio between the distance S_i from the focusing element (the main lens in standard plenoptic, the source in CPI) to the image plane, and the distance S_i' between the focusing element and the detector. Perfect refocusing is possible when [2]:

$$\left|1 - \frac{1}{\alpha}\right| < M\frac{\delta_x}{\delta_u} = \frac{\Delta x}{\Delta u}, \quad (12)$$

where $\Delta x = 2\delta_x$ is the minimum distance that can be resolved on the image plane, and $\Delta u = 2\delta_u/M$ is the minimum distance that can be resolved on the focusing element, with M the latter's magnification. Now, in standard PI, the image resolution is given by the width of the macropixel $\Delta x^{(p)} = 2\delta N_u^{(p)}$, while each (micro)pixel δ coincides with a region on the lens plane of width $\Delta u^{(p)} = 2D_s/N_u^{(p)}$; hence,
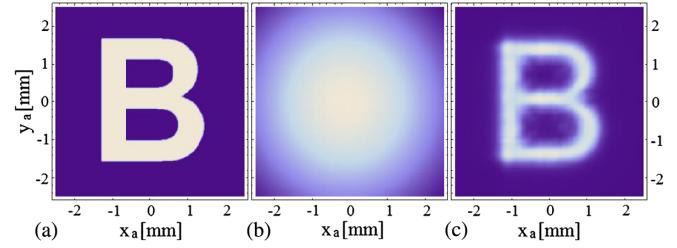

FIG. 3.   Simulations of a CPI system illuminated by a chaotic source with $\lambda = 500$ nm and a Gaussian intensity profile of width $D_s \simeq 3\sigma = 1.8$ mm; the source is magnified by $M = 0.8$, the pixel size is $\delta = 32$ μm, the number of pixels for spatial and directional resolutions are $N_x^{(\text{cp})} = N_u^{(\text{cp})} = 150$. (a) Focused image in $z_a = z_b = 10$ mm. (b) Out-of-focus correlation image retrieved in $z_a = 10$ mm, with $z_b = 50$ mm. (c) Refocused image as given by Eq. (11).

$$\left(\frac{\Delta x}{\Delta u}\right)^{(p)} = \frac{\delta}{D_s}(N_u^{(p)})^2. \quad (13)$$

In CPI, the relation $\Delta u^{(\text{cp})} = 2D_s/N_u^{(\text{cp})}$ is unchanged, but $\Delta x^{(\text{cp})} = 2\delta$, since pixels of width δ can be used also to retrieve the image. Hence,

$$\left(\frac{\Delta x}{\Delta u}\right)^{(\text{cp})} = \frac{\delta}{D_s}N_u^{(\text{cp})}. \quad (14)$$

In conclusion, CPI enables to extend perfect refocusing at a much longer distance with respect to PI, since

$$\frac{\text{DOF}^{(\text{cp})}}{\text{DOF}^{(p)}} = \frac{N_u^{(\text{cp})}}{(N_u^{(p)})^2} \quad (15)$$

can be easily made larger than one in experiments.

Based on Eq. (12), in the simulation reported in Fig. 3, the maximum object distance for perfect refocusing is $z_b = 5z_a$. For the given total number of pixels per side $N_{\text{tot}} = 300$, a PI system with the same spatial resolution $N_x^{(p)} = 150$, would lead to an angular resolution of $N_u^{(p)} = N_{\text{tot}}/N_x^{(p)} = 2$. Based on Eq. (15), the CPI system enables refocusing at a depth of focus that is almost 40 times higher than for the equivalent PI system.

Conclusions and outlook.—We have presented an innovative approach to plenoptic imaging which exploits the fundamental correlation properties of chaotic light to decouple spatial and angular resolution of standard imaging systems. This has enabled us to perform plenoptic imaging at a significantly higher depth of field with respect to an equivalent standard plenoptic imaging device. As plenoptic imaging is being broadly adopted in diverse fields such as digital photography [3], microscopy [10,11], 3D imaging, sensing, and rendering [4], our proposed scheme has direct applications in several biomedical and engineering fields. We have analyzed the CPI setup as an imaging device; potentially, it would also represent an interesting tool to characterize turbulence, thus enabling volumetric imaging within scattering media [5]. Interestingly, the coherent nature of the correlation plenoptic imaging technique

may lead to innovative coherent microscopy modality. The merging of plenoptic imaging and correlation quantum imaging has thus the potential to open a totally new line of research and pave the way towards the promising applications of plenoptic imaging.

In view of practical applications, it is worth mentioning that the obtained results do not depend on the nature of the object, whether reflective or transmissive. It is also reasonable to expect the CPI procedure to work with any source, of either photons or particles [32], that is characterized by correlation in *both* momentum *and* position [17,18]. In particular, when replacing the chaotic source with an entangled photon source such as Spontaneous Parametric Down-Conversion [33], the light source can still be imaged on D_b to obtain the angular information, but a lens is required to achieve ghost imaging of the object [16,18]. On the contrary, we do not expect CPI to work with classically correlated beams of the kind employed in Ref. [34], which are only characterized by momentum correlation [18].

---

[*]milena.dangelo@uniba.it

[†]francesco.pepe@ba.infn.it

[1] E. H. Adelson and J. Y. A. Wang, IEEE Trans. Pattern Anal. Mach. Intell. **14**, 99 (1992).

[2] R. Ng, M. Levoy, M. Brédif, G. Duval, M. Horowitz, and P. Hanrahan, Technical Report CSTR 2005-02, Stanford Computer Science, 2005.

[3] https://www.lytro.com/illum; http://www.raytrix.de/; http://www.pelicanimaging.com.

[4] X. Xiao, B. Javidi, M. Martinez-Corral, and A. Stern, Appl. Opt. **52**, 546 (2013).

[5] H. Liu, E. Jonas, L. Tian, Z. Jingshan, B. Recht, and L. Waller, Opt. Express **23**, 14461 (2015).

[6] S. Muenzel and J. W. Fleischer, Appl. Opt. **52**, D97 (2013).

[7] M. Levoy and P. Hanrahan, Proceedings of SIGGRAPH '96 (New Orleans, LA, August 4–9, 1996), *Computer Graphics Proceedings*, Annual Conference Series (ACM SIGGRAPH, 1996), pp. 31–42.

[8] M. Levoy, R. Ng, A. Adams, M. Footer, and M. Horowitz, ACM Trans. Graph. **25**, 924 (2006).

[9] W. Glastre, O. Hugon, O. Jacquin, H. Guillet de Chatellus, and E. Lacot, Opt. Express **21**, 7294 (2013).

[10] M. Broxton, L. Grosenick, S. Yang, N. Cohen, A. Andalman, K. Deisseroth, and M. Levoy, Opt. Express **21**, 25418 (2013).

[11] R. Prevedel, Y.-G. Yoon, M. Hoffmann, N. Pak, G. Wetzstein, S. Kato, T Schrödel, R. Raskar, M. Zimmer, E. S. Boyden, and A. Vaziri, Nat. Methods **11**, 727 (2014).

[12] L. Waller, G. Situ, and J. W. Fleischer, Nat. Photonics **6**, 474 (2012).

[13] T. Georgeiv, K. C. Zheng, B. Curless, D. Salesin, S. Nayar, and C. Intwala, Spatio-Angular Resolution Tradeoff in Integral Photography, in Eurographics Symposium on Rendering, 2006 edited by T. Akenine-Möller, and W. Heidrich (The Eurographics Association, Geneva, 2006).

[14] S. A. Schroff and K. Berkner, Appl. Opt. **52**, D22 (2013).

[15] J. Pérez, E. Magdaleno, F. Pérez, M. Rodríguez, D. Hernández, and J Corrales, Sensors **14**, 8669 (2014).

[16] T. B. Pittman, Y. H. Shih, D. V. Strekalov, and A. V. Sergienko, Phys. Rev. A **52**, R3429 (1995); T. B. Pittman, D. V. Strekalov, D. N. Klyshko, M. H. Rubin, A. V. Sergienko, and Y. H. Shih, Phys. Rev. A **53**, 2804 (1996).

[17] A. Gatti, E. Brambilla, M. Bache, and L. A. Lugiato, Phys. Rev. A **70**, 013802 (2004).

[18] M. D'Angelo and Y. H. Shih, Laser Phys. Lett. **2**, 567 (2005).

[19] A. Valencia, G. Scarcelli, M. D'Angelo, and Y. H. Shih, Phys. Rev. Lett. **94**, 063601 (2005).

[20] G. Scarcelli, V. Berardi, and Y. H. Shih, Phys. Rev. Lett. **96**, 063602 (2006).

[21] F. Ferri, D. Magatti, A. Gatti, M. Bache, E. Brambilla, and L. A. Lugiato, Phys. Rev. Lett. **94**, 183602 (2005).

[22] S. Mancini, V. I. Man'ko, and P. Tombesi, Phys. Lett. A **213**, 1 (1996).

[23] A. I. Lvovsky and M. G. Raymer, Rev. Mod. Phys. **81**, 299 (2009).

[24] Whenever, for practical purposes, the image needs to be reproduced at a distance from the source different from the object distance z_b, a lens must be introduced at a distance s_i from detector D_a such that $1/(z_a - z_b) + 1/s_i = 1/f$, where z_a is the distance of the lens from the source and f is the lens focal length [19]. This enables displacing the correlation image of the object, obtained at a distance z_b from the source, to any convenient location, without changing the physics and the effectiveness of the CPI scheme.

[25] G. Brida, M. V. Chekhova, G. A. Fornaro, M. Genovese, E. D. Lopaeva, and I. Ruo Berchera, Phys. Rev. A **83**, 063807 (2011).

[26] With a sCMOS camera with full well capacity 3×10^4 electrons/s and acquisition time 5 ms for a 10^6 pixel image, one needs a photon rate at the camera of 40000 s^{-1}. This can be easily achieved with any pseudothermal source made of a laser beam impinging on a moving scattering medium or a spatial light modulator. In the case of low power, a chaotic source such as a LED with wavelength $\lambda = 630$ nm and FWHM 20 nm needs to be filtered to a FWHM of about $10^{(-10)}$ nm to match the bandwidth of the camera; hence, the required power of the LED is of the order of 1 mW. The constraint on the source bandwidth can be released when high power is available (see Fig. 3 in Ref. [25]). Also in this case, even considering collection losses, both pseudothermal sources and ultra-high-power LEDs available on the market ($P = 700$ mW) represent realistic sources for implementing CPI.

[27] M. O. Scully and M. S. Zubairy, *Quantum Optics* (Cambridge University Press, Cambridge, 1997).

[28] J. W. Goodman, *Introduction to Fourier Optics* (McGraw-Hill, New York, 1996).

[29] In a realistic situation, such as the one in Fig. 3, with a reasonable source power and camera [26], the total acquisition

time is around 25 s for 5000 acquisitions for a 10^6 pixels image, which can go down to about 2 s for a 128×128 pixels image. This time can be reduced by implementing compressed sensing techniques (see, e.g., Ref. [30]).

$$\boldsymbol{\rho}_o = \frac{z_a}{z_b}\boldsymbol{\rho}_a - \frac{\boldsymbol{\rho}_b}{M}\left(1 - \frac{z_a}{z_b}\right), \qquad \boldsymbol{\rho}_s = -\frac{\boldsymbol{\rho}_b}{M},$$

thus justifying the intuitive result of Eq. (10).

[30] Liu Jiying, Zhu Jubo, Lu Chuan, and Huang Shisheng, Opt. Lett. **35**, 1206 (2010).

[31] The result of Eq. (10) can be formally obtained from Eq. (5) by considering the stationary-phase approximation of the integrand in the limit $\omega \to \infty$. In fact, in this limit, the most prominent contribution to the integral comes from vanishingly small regions around the points

[32] M. D'Angelo, A. Garuccio, F. Romano, F. Di Lena, M. D'Incecco, R. Moro, A. Regano, and G. Scarcelli, Springer Proc. Phys. **145**, 237 (2014).

[33] D. N. Klyshko, *Photons and Nonlinear Optics* (Gordon and Breach, New York, 1988).

[34] R. S. Bennink, S. J. Bentley, and R. W. Boyd, Phys. Rev. Lett. **89**, 113601 (2002).